

# Field Trial: Demonstrating Automatic Reconfiguration of Optical Networks Based on Finite State Machine

Nicola Sambo<sup>1</sup>, Kostas Christodoulopoulos, Nikos Argyris<sup>2</sup>, Pietro Giardina, Camille Delezoide<sup>3</sup>, Diego Roccato, Alessandro Percelsi, Roberto Morro<sup>4</sup>, Andrea Sgambelluri<sup>5</sup>, Aristotelis Kretsis<sup>6</sup>, Giannis Kanakis<sup>7</sup>, Giacomo Bernini, Emmanuel Varvarigos, and Piero Castoldi<sup>8</sup>

(Invited Paper)

**Abstract**—Optical networks are evolving toward self-adaptation exploiting self-observation of network conditions (e.g., through monitoring at the physical layer). Thus, according to monitoring information, reconfiguration of network devices including switches and transponders (e.g., transmission parameters) is acted. Typically, the network is thought as centralized, where a central software defined networking (SDN) controller holds the overall view of network topology and resources and, upon connection request, it decides for routing and spectrum assignment, and, then, it configures accordingly the data plane. Similarly, the central controller receives notifications when failures occur and (re)acts by reconfiguring the data plane. However, centralized solutions can suffer from scalability and responsiveness issues, translating in delays during provisioning and recovery. In this paper, we report the demonstration in a field trial of an automatic and self-reconfigurable network. We leverage a novel control paradigm based on programmable finite state machine where each state is associated to a specific network condition and a state transition implies network reconfiguration. Thanks to this approach the central controller can instruct (pre-program) network devices making them aware of the proper reconfiguration settings associated to the network conditions. Then, the reconfiguration is triggered locally, thus increasing scalability

and response speed. Two successful experiments will be shown: first, local transmission parameter adaption according to physical layer conditions; second, connection central frequency optimization mitigating filtering effects and distortions.

**Index Terms**—Network automation, NETCONF, recovery, self-adaptation, self-reconfiguration, YANG.

## I. INTRODUCTION

THE continuous growth of IP traffic, the emergence of new services and the future introduction of 5G motivate the design of a new truly flexible and programmable network. Typically, optical connections—lightpaths—are overprovisioned for both physical layer attributes and capacity, and remain unchanged for several years. The current practice in the physical layer is to estimate the lightpaths' Quality of Transmission (QoT) with high margins to achieve uninterrupted network operation until End-of-Life (EOL) [1], [2]. Reducing the margins (e.g., to account for ageing and QoT estimation inaccuracy) can yield significant cost savings [2], for this reason margin reduction has been recently investigated [1]–[4].

To enable an agile optical network that operates efficiently, with reduced margins, throughout its lifetime and is able to resolve critical performance degradations (e.g., because of the increase of noise figure of amplifiers due to ageing), the feedback from the physical layer is crucial [5]–[10]. In particular, we refer to *soft failures* as performance degradations of network devices such as fibers, amplifiers, filters, and so on, which in turns imply a QoT deterioration (e.g., bit error rate—BER—increase) of the signals exploiting those devices. Such problems become critical when performance parameters exceed some thresholds (e.g., on BER) and can be in several cases overcome by readapting transmission parameters (e.g., modulation format) to make transmission more robust to physical layer impairments [5]. The efficient observation of the network—which currently can exploit monitors embedded in coherent transponders—is essential to understand the actual conditions (e.g., used for improving the accuracy of QoT estimation [11]—when establishing new lightpaths or reconfiguring existing ones) and also to trigger network re-adaptation upon soft failures [5], [6]. So, the management of

Manuscript received December 12, 2018; revised May 13, 2019; accepted June 11, 2019. Date of publication June 14, 2019; date of current version July 31, 2019. This work was supported by the EC through the Horizon 2020 ORCHESTRA project (g.a. 645360). This paper was presented in part at OSA Photonic Networks and Devices Conference, Zurich, Switzerland, July 2018. (Corresponding author: Nicola Sambo.)

N. Sambo, A. Sgambelluri, and P. Castoldi are with the Scuola Superiore Sant'Anna, Pisa 56127, Italy (e-mail: nicola.sambo@santannapisa.it; a.sgambelluri@sssup.it; castoldi@sssup.it).

K. Christodoulopoulos was with the CTI, Patras 26504, Greece. He is now with the Nokia Bell Labs, Stuttgart 70435, Germany (e-mail: konstantinos.l.christodoulopoulos@nokia-bell-labs.com).

N. Argyris and G. Kanakis are with the National Technical University of Athens, Athens 15780, Greece (e-mail: nikosa@mellanox.com; giankan@mail.ntua.gr).

P. Giardina and G. Bernini are with the Nextworks, Pisa 56122, Italy (e-mail: p.giardina@nextworks.it; g.bernini@nextworks.it).

C. Delezoide is with the Nokia Bell Labs, Paris 91620, France (e-mail: camille.delezoide@nokia-bell-labs.com).

D. Roccato, A. Percelsi, and R. Morro are with the TIM, Torino 10121, Italy (e-mail: diego.roccato@telecomitalia.it; alessandro.percelsi@telecomitalia.it; roberto.morro@telecomitalia.it).

A. Kretsis and E. Varvarigos are with the CTI, Patras 26504, Greece (e-mail: akretsis@ceid.upatras.gr; vmanos@central.ntua.gr).

Color versions of one or more of the figures in this paper are available online at <http://ieeexplore.ieee.org>.

Digital Object Identifier 10.1109/JLT.2019.2922841

monitoring and alarms becomes a relevant task in low-margins networks, because monitoring information can be large and several alarms can be generated [12]. Indeed, more alarms are expected in margin-less network operation than in traditional networks. Then, a scalable management of monitoring is required because recovery (e.g., re-routing or adaptation of transmission parameters [12]) is triggered upon processing of such information. In other words, inefficient management can yield delays in the recovery due to the queuing time when processing alarms.

Recently, a new paradigm of recovery scheme (named *pre-programming*) exploiting monitoring information was proposed [13]. Pre-programming was designed to react against soft-failures. According to this scheme, the SDN controller pre-computes the type of recovery consisting in transmission parameter adaptation (e.g., change of modulation format or code) for a given soft failure. Then, the SDN controller instructs the transponders about the action(s) to perform in case of degradation, while the lightpath is still active. Instructions are given in the form of a *finite state machine (FSM)* through the NETCONF protocol and a properly designed YANG model reflecting the FSM. When the degradation occurs, the transponder promptly reacts by self-reconfiguring the proper transmission parameters without asking and waiting for computations from the SDN controller. The FSM can consider one or several monitored parameters, have few or several states and simple or more complicated transition rules to cover various factors according to the use case at hand. It can also include an “alarm” state, which would cover events that were not taken into account in the FSM. When this state is reached an alarm is created including monitoring information. The alarm is forwarded to the controller that then is charged to resolve the problem (e.g., with rerouting).

The proposed solution is a sort of hybrid centralized/distributed control scheme since instructions are decided centrally but are acted in a distributed way by devices when the problem appears. Such an approach is different than other hybrid centralized/distributed solutions proposed in the past, as an example, based on Path Computation Element (PCE) and Generalized Multi-Protocol Label Switching (GMPLS) [14]–[17]. Indeed, differently than those solutions, pre-programming permits to easily re-program the reactions of devices. GMPLS does not provide such flexibility since the protocols of the GMPLS suite are based on bit encoding. This strongly limits the programmability of the network because if new events have to be considered and new reconfigurations implemented, the protocol messages’ content (such as header and objects) should be redesigned [13]. On the contrary, thanks to the nature of YANG, the FSM model can be refined without redesigning the NETCONF protocol, thus providing a much more effective solution with respect to bit encoding. This makes pre-programming suitable for re-program network devices even according to new policies and network conditions to be taken into account. An activity within the Internet Engineering Task Force (IETF) is evaluating several use cases of application for FSM [18]: telemetry, performance monitoring based on network clusterization, besides transmission adaptation as in this paper. Moreover, the proposed approach, being based on NETCONF, is compliant

with networks controlled through this protocol, which is going to be widely considered by operators and vendors (e.g., in disaggregated networks [19], [20]). Pre-programming was evaluated and shown to achieve faster recovery against a fully centralized environment [21].

In this paper, we demonstrate the automatic reconfiguration of an optical network, based on FSM, in a field trial at TIM, Torino, Italy, exploiting an offline coherent receiver. The paper is an extended version of [22]. In this paper, we provide more details about the FSM-based control and the field trial. In addition, we report on the integration between the FSM-based control plane and TIM control plane. Moreover, we introduce a new use case and present the related demonstration in TIM network. This new use case involves the tuning of the central frequency associated to an optical connection in order to mitigate filtering impairments when lasers or wavelength selective switches (WSS) experience a drift (e.g., due to ageing). The successful experiments demonstrate for the first time the feasibility of the FSM-based control in a real environment.

## II. PROGRAMMING NETWORK RECONFIGURATION WITH FINITE STATE MACHINE

In this paper, we will focus on two main applications of finite-state-machine (FSM)-based control. The first one consists on pre-programming the transponder on modulation format to be used depending on the physical layer conditions. During the field trial, the reconfiguration was done locally at the transponder without intervention of the central controller when physical layer changes are sensed/detected by the transponder at hand. The second application involves the optimization of the connection central frequency upon drifts of the laser or filters along the path with the aim of mitigating filter distortions. In this case, during the field trial, the reconfiguration was acted by the central controller and not locally. However, even this solution has the prospects to be implemented locally at the transponder and this will be the focus of future studies. The proposed FSM based control scheme is generic and applicable to short, medium and long-term use cases. The field experiments, performed as a proof of concept for the scheme and reported in Section IV, target the recovery from medium to long-term effects. In particular, they consider the deterioration of performance due to increased noise and the detuning of lasers and filters that typically arise due to long-term ageing. The proposed control scheme could be applied to cover shorter time effects with more and fine-grained states according to the equipment specifications, monitoring accuracy, and the particularities of the targeted application.

### A. Pre-Programming Based on Modulation Format and Bit Rate Adaption

The pre-programming of the modulation format settings is done for two purposes: i) to react against soft-failures and ii) to apply low margins. In the former, the network conditions degrade, thus pre-programming acts a network reconfiguration for survivability purposes: as an example, by changing the modulation format from a more spectral efficient (e.g., polarization multiplexing 8 quadrature amplitude modulation–PM-8QAM)

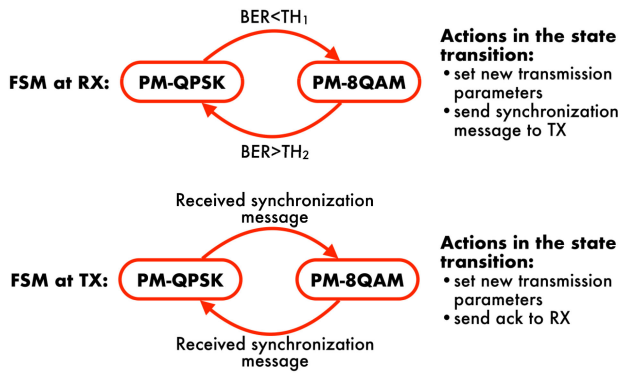


Fig. 1. Pre-programming recovery based on modulation format adaptation.

to a more robust one against transmission impairments (e.g., PM-quadrature phase shift keying–PM-QPSK). Differently, in the latter case of low-margin application, a given BER is estimated for the considered path but the monitoring system reveals that the estimation is pessimistic and the actual physical conditions enable a more spectral efficient modulation format. Thus, pre-programming acts a reconfiguration from PM-QPSK to PM-8QAM. We consider these two modulation formats since they were the ones available during the field trial. Note that when operating at fixed symbol rate –28 GBaud – the use of a different modulation format implies a different gross bit rate, i.e., 112 Gb/s with PM-QPSK and 168 Gb/s with PM-8QAM.

Such reconfigurations are based on FSM. One or more FSMs are associated to an active optical connection and installed (through a NETCONF <edit-config> message based on the YANG model for FSM [13]) at the transmitter (TX) and at the receiver (RX) ends. The FSMs for pre-programming based on modulation format adaptation are shown in Fig. 1. This way, a transponder is aware of the modulation format to self apply based on the physical layer conditions that it observes.

In Fig. 1, each state of the FSM is associated to a specific configuration of transmission parameters. Assume that a QoT estimation tool adopting network margins (e.g., considering a penalty due to ageing) estimates that the acceptable modulation format for the connection is PM-QPSK (thus 100 Gb/s net rate), not PM-8QAM. The PM-QPSK lightpath is established and coherently received at RX, which embeds a BER monitor. Both TX and RX are in the “PM-QPSK” state of the FSM. The monitoring system reveals that PM-8QAM is acceptable (BER < TH<sub>1</sub>), a higher margin is actually available and can be reduced when adapting to PM-8QAM (thus, 150 Gb/s net rate). Consequently, reconfiguration is triggered at RX, which informs TX about the change of transmission parameters through a synchronization message along the supervisory channel. At TX, the reception of this message triggers the change of transmission parameters. TX acknowledges RX about the change. Both TX and RX are now in the “PM-8QAM” state.

Similarly, when the FSMs are in the “PM-8QAM” state and a soft failure occurs, if the RX reveals a BER > TH<sub>2</sub>, a state transition is triggered and the transmission passes from PM-8QAM (150 Gb/s net rate) to PM-QPSK (100 Gb/s net rate). The change of modulation format implies a bit rate reduction. As shown in [21], given the faster recovery achieved by pre-programming

with respect to a fully centralized approach, higher-priority traffic can be recovered with pre-programming while lower-priority traffic through rerouting performed by the SDN controller. Moreover, we have to note that, with pre-programming, a less amount of traffic (only low priority) has to be handled by the central controller, thus reducing the processing time and queuing delay for recovery. This brings also benefits to low priority traffic with respect to a fully centralized approach, as demonstrated in [21].

Note that the proposed control scheme can be also applied to other transmission techniques, such as probabilistic shaping [23] or time frequency packing [24]. Given a modulation format, such techniques permit to further increase the information rate depending on the actual optical signal to noise ratio (OSNR), mainly impacting the type of adopted code and the code rate. Pre-programming, if applied to such transmission techniques, should encompass proper state transitions associated to specific OSNR levels, e.g., each one driving an appropriate “shaping” of the constellation. Specifically, depending on the monitored OSNR, the reaction should imply the configuration of attributes related to the code, code rate, and modulation format of the YANG model describing the transponder. An example of transponder YANG model is reported in [25], for instance including the attribute <rate> referred to the code. Please, note that also in this paper, the code is actually configured.

Finally, as outlined above, it may happen that a degrading event has not been taken into account into the FSM. Thus, in order to guarantee the maintenance of the service, a specific state named “alarm” can be included in the FSM, and the action to be taken is to send an alarm (reporting the values of the monitored parameters) to the SDN controller, which will take in charge the maintenance of the signal, e.g., by relying on rerouting.

### B. Pre-Programming for Central Frequency Re-Tuning

It may happen that a lightpath does not experience the best achievable QoT because of misalignments with filters along the path. This can be due to laser drifting at TX, or at the local oscillator at RX, or to filters misalignments, in general. This way, the cascade of several filters creates narrowing and a tilting of the spectrum. In such a case, by aligning the TX/RX with the filters, a better QoT can be achieved. In general, the process of optimizing the TX/RX frequency to align with the filters can be done while the network operates, periodically or on demand, but can also be a reaction that is applied when a soft failure occurs. The TX/RX central frequency is moved by a certain step  $\Delta f$  (e.g., 1 GHz) while one or more indicative parameters (e.g., BER) are in a given range. Depending on these parameters the system also decides to move in a direction or towards the other direction in the spectrum. This is decided based on the previous monitored values of the indicative parameters. The step should be chosen according to the accuracy of the monitoring parameters that are used, which in turn also defines the optimization accuracy that we can achieve. This optimization procedure can be described with a FSM.

Fig. 2 shows the FSM for central frequency optimization, considering a lightpath that initially is at  $f_0$ . When, the SDN controller triggers reconfiguration, the state passes to “Attempt

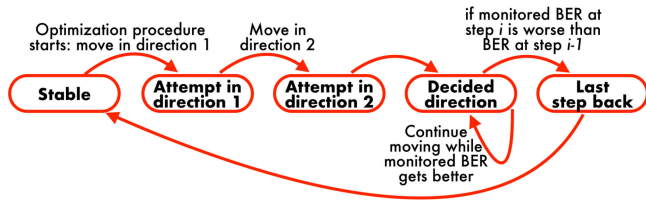


Fig. 2. Optimization of central frequency FSM.

in direction 1” state. So, the SDN controller changes the central frequency  $f_0$  of TX by  $-\Delta f$ . Thanks to the automatic frequency control natively installed at the coherent receiver, RX is able to follow this change while traffic is transmitted without the use of any control message and without any loss of traffic (as it happens for the push-pull [26]). In this state, BER is monitored and its value is sent to the SDN controller. The FSM moves to “Attempt in direction 2”, where the frequency  $f_0 + \Delta f$  is configured. BER is monitored and passed again to the SDN controller. The state passes to “Decided direction” state. At this stage the direction is decided depending on the measured BER at  $+\Delta f$  and  $-\Delta f$ . The direction with the lowest BER is selected. In this state, the central frequency is incremented (or decremented, depending on the decided direction) step by step by  $\Delta f$  while the monitoring system reports a BER decrease. When BER increases (i.e., BER at step  $i$  is higher than BER at step  $i - 1$ ), the signal has been shifted too much. In this case, at the state “Last step back” the central frequency is reported to its value at the step  $i - 1$  and BER re-verified. Then, the optimization procedure terminates and the FSM returns to the “stable” state. In our demonstration (Section IV) this process was centrally implemented, but, as stated before, it can be implemented locally through the installation of the related FSM, as done for modulation format adaptation.

The frequency alignment process discussed above can be improved. One idea is to use a variable step that is large in the beginning and is adapted/reduced as we move towards the optimum alignment. We can also measure / monitor more parameters than only the BER and use those to improve our decisions regarding the direction and the step. For example, [27] proposes to measure the signal-filter detuning from the signal power spectral density. Such optimization intelligence can be translated into an appropriate FSM and pre-programmed to be performed locally with the proposed control plane scheme.

### III. CONTROL AND MANAGEMENT PLANE ARCHITECTURE EXPLOITED IN THE FIELD TRIAL

This section introduces the control and management plane exploiting FSM integrated in the TIM optical network employing commercial reconfigurable optical add&drop multiplexers (ROADMs) and custom-built flexible transponders [28] (supporting the configuration of transmission parameters such as bit rate, symbol rate, code, modulation format, central frequency, and power). More specifically, this section will present the integration of the proposed new control features with the control plane at TIM to enable the field trial.

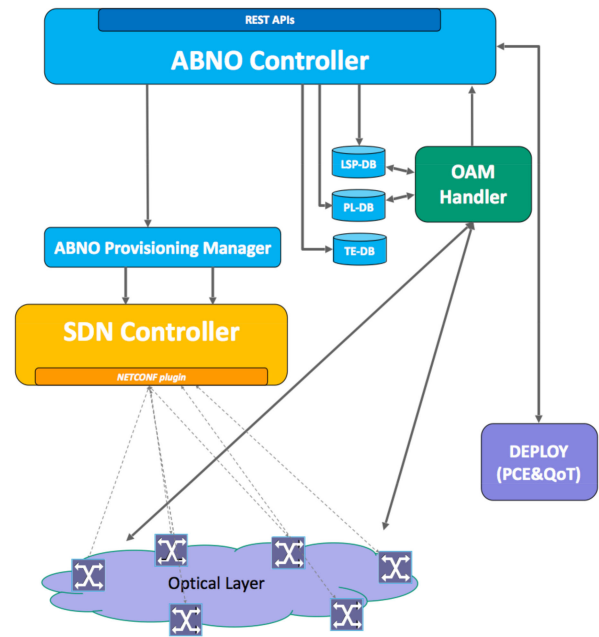


Fig. 3. Control plane architecture.

#### A. Main Architecture

Fig. 3 shows the control and management plane architecture employed in the field trial. The architecture is based on the Application-Based Network Operations (ABNO) functional modules [29] that provide an abstraction of relevant control and management tasks such as provisioning, path computation, operation, administration, and maintenance. The ABNO-controller governs the modules that implement these functions. Routing and Spectrum Assignment (RSA), which is QoT-aware, is performed by the DEPLOY Path Computation Element (PCE), as in [30]. DEPLOY exploits: Traffic Engineering Database (TED), Physical Layer-DataBase (PL-DB) including nominal, estimated, and monitored physical layer parameters, and Label Switched Path DB (LSP-DB) including state information of lightpaths. Besides RSA, DEPLOY also decides transponder configuration parameters (symbol rate, code rate, and modulation format) based on the physical layer. Then, the ABNO controller triggers the Provisioning Manager to configure the data plane using NETCONF protocol [31]. The Provisioning Manager integrates an SDN controller, which actually configures the network. The YANG model detailed in [21] is adopted to describe flexible transponders, while the YANG model in [5] is considered for bandwidth variable wavelength selective switch (BV-WSS) describing the central frequency and bandwidth of the switched signal through the ITU-T  $n$  and  $m$  parameters [32]. The Operation Administration and Maintenance (OAM) Handler processes monitoring information or notifications from monitors (as the monitored BER during central frequency optimization), and it is responsible for service maintenance. The NETCONF `<edit-config>` message is sent by the Provisioning Manager to configure transponders and BV-WSSs. The NETCONF `<edit-config>` message is also used by the SDN

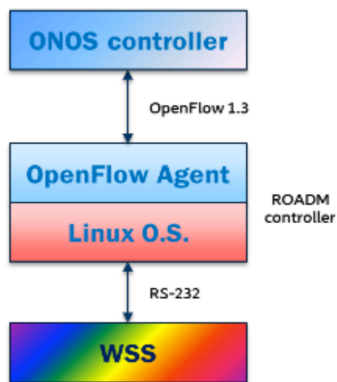


Fig. 4. Control of a TIM ROADM.

controller to install FSMs in the transponder, thus enabling pre-programming. The NETCONF <notification> is exploited to send monitored parameters to the OAM Handler, as in the case of central frequency optimization, or to notify the accomplishment of a pre-programmed reconfiguration. For a more detailed description of NETCONF messages the reader can refer to [31].

### B. Integration Between the Adopted Control Plane and the TIM Control Plane

For the purpose of this field trial it was necessary to extend the ABNO Provisioning Manager in order to integrate and interface with the Open Network Operating System (ONOS) SDN Controller used by TIM to control their ROADM nodes. This allowed to exploit Provisioning Manager as plugin-based translator and adapter of ABNO, SDN models and procedures, and pre-programming. Fig. 4 shows a schematic representation of TIM ROADM control: an OpenFlow [33] agent—running on a Linux box (on Ubuntu and Fedora) and developed in C language—is in charge of managing the OpenFlow session with the SDN controller, creating and releasing cross-connections under controller request and keeping the status of the ports and connections. The agent is compliant with OpenFlow version 1.3 and with the Optical Transport extensions described in the document ONF TS-022 [34]. Those extensions allow the creation of a media channel (i.e., a connection) between a device connected to an input port and an output port of the ROADMs specifying channel central frequency, channel width and channel spacing. ONOS 1.11 [37] is used as SDN controller of the ROADMs.

In the context of the field trial, a new dedicated ONOS plugin was implemented in the ABNO Provisioning Manager, in addition to the NETCONF one, as shown in Fig. 5, in order to apply configurations, reconfigurations and deletion of cross-connections into the ONOS-controlled TIM ROADMs. This ONOS plugin implements the client side of the ONOS Flows management application programming interfaces (APIs) [35], enhanced for the management of optical resources and ROADMs. These APIs are based on REST [36] with the exchange of JavaScript Object Notation (JSON) messages that follows the ONOS information model. As an example, Fig. 6 and Fig. 7 show an interaction between the ABNO Provisioning

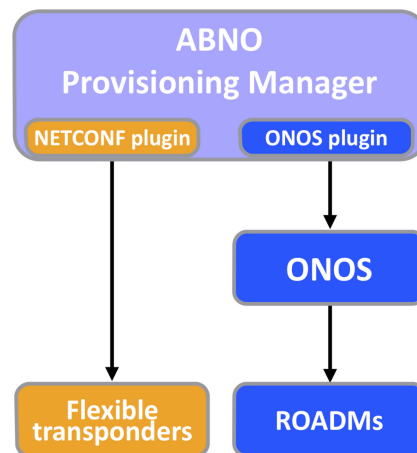


Fig. 5. ONOS plugin in the Provisioning Manager.

```

2017-12-13 18:12:21,278 DEBUG OnosPlugin:172 - Going to configure node
2 through ONOS
2017-12-13 18:12:21,284 INFO OnosPlugin:196 - Message to ONOS is:
{
  "flows": [ {
    "priority": 40000,
    "isPermanent": true,
    "deviceId": "of:000100306db646e4",
    "selector": {
      "criteria": [ {
        "port": 1,
        "type": "IN_PORT"
      } ],
      "ochSignalType": "FLEX_GRID",
      "type": "OCH_SIGTYPE"
    }, {
      "ochSignalId": {
        "gridType": "FLEX",
        "channelSpacing": "CHL_6P25GHZ",
        "spacingMultiplier": 80,
        "slotGranularity": 3
      },
      "type": "OCH_SIGID"
    }
  ]
}, {
  "treatment": {
    "instructions": [ {
      "port": 4,
      "type": "OUTPUT"
    } ]
  }
} ]
}

```

Fig. 6. JSON request message sent by ABNO to ONOS to provision a cross-connection.

```

2017-12-13 18:12:21,296 INFO OnosPlugin:208 - ONOS response is:
{
  "flows": [ {
    "deviceId": "of:000100306db646e4",
    "flowId": "32932574621339546"
  } ]
}

```

Fig. 7. JSON response message sent by ONOS to ABNO to acknowledge the provisioning of a cross-connection.

Manager and the ONOS SDN Controller (as extracted from the ABNO log files) for the provisioning of a cross-connection in one of the TIM's ROADM. In particular, as shown in Fig. 6, a cross connection is requested from the input port 1 to the output

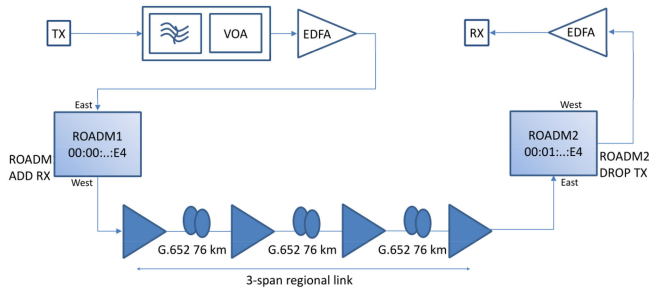


Fig. 8. Field trial data plane.

port 4, where “spacingMultiplier” and “slotGranularity” correspond to the ITU-T  $n$  and  $m$  parameters, respectively. Fig. 7 shows the related response.

#### IV. FIELD TRIAL IN TIM AND EXPERIMENTAL DEMONSTRATION

The setup shown in Fig. 8 was exploited for the field trial in TIM. The custom-built transponder (TX and RX) supports PM-8QAM and PM-QPSK modulation formats in a single carrier scheme, with 150 and 100 Gb/s respective net rates, 12% and 28% code rate, 28 and 32 Gbaud. The Rx provides end-to-end monitor of SNR, OSNR, group velocity delay (GVD), polarization mode dispersion (PMD), and BER. A tunable optical filter (TOF) is placed after the TX to emulate impairments due to laser and filter misalignment in a cascade of filters (e.g., due to laser aging). The variable optical attenuator (VOA) placed after the TOF is used to induce attenuation increase along the link impacting the signal OSNR. Then, the signal, after being amplified by an EDFA, enters the ROADM1 and is transmitted through the 3-span optical regional link. An optical spectrum analyzer (OSA) monitors the optical spectrum of the signals at the exit from the regional link. After the propagation through the link, the signal is dropped at ROADM2, optically pre-amplified and delivered to RX. BER is measured offline over  $4 \times 10^4$  symbols per minute.

First, pre-programming is demonstrated for modulation format adaptation and, then, central frequency optimization is shown.

##### A. Modulation Format Adaptation to Reduce Margins or to React to a Soft Failure

Prior to this experiment, we trained the QoT estimator residing in DEPLOY of ABNO controller (Fig. 3) to be able to translate between BER and OSNR values for the supported modulation formats and symbol rates of the TR/RX. We initially established the lightpath at 100G-QPSK and we monitored it for a short period, i.e., days-weeks in the real world (minutes in lab), so that we observed and learned the average and standard deviation of the BER. These are natural fluctuations due to short-term effects, such as polarization impairments, etc. Based on these measurements we defined a *hysteresis* margin to avoid switching from one modulation format to another due to natural short-term performance fluctuations. Then based on the BER-OSNR fitted functions, the hysteresis margin, and any additional OSNR

```

<finite-state-machine xmlns="http://sssup.it/fsm">
  <current-state>1</current-state>
  <states>
    <state>
      <id>1</id>
      <description>pm-qpsk</description>
      ...
      <name>BER</name>
      <type>ev:ON_CHANGE</type>
      <threshold-param>0.000058</threshold-param>
      <check-operator>LT</check-operator>
      <reaction>
        <operation>
          ...
          <config>
            <bit-rate>150</bit-rate>
            <baud-rate>32.0</baud-rate>
            <modulation xmlns:mf="http://sssup.it/modulation-formats">
              mf:pm-8qam
            </modulation>
          </config>
          ...
        </operation>
      </reaction>
    </state>
    <state>
      <id>2</id>
      <description>pm-8qam</description>
      ...
      <name>BER</name>
      <type>ev:ON_CHANGE</type>
      <threshold-param>0.0199781</threshold-param>
      <check-operator>GT</check-operator>
      <reaction>
        <operation>
          ...
          <config>
            <bit-rate>100</bit-rate>
            <baud-rate>32.0</baud-rate>
            <modulation xmlns:mf="http://sssup.it/modulation-formats">
              mf:pm-qpsk
            </modulation>
          </config>
          ...
        </operation>
      </reaction>
    </state>
  </states>
</finite-state-machine>

```

Fig. 9. Finite state machine (FSM) installed at RX for modulation format adaptation.

margin required (set to 0 in our experiments), we calculated the BER thresholds to upgrade from QPSK to 8QAM and the opposite. In this experiment, if the transponder is configured with PM-QPSK and the monitored BER at the receiver is below  $5.8 \times 10^{-5}$ , the transponder self-reconfigures the modulation format to PM-8QAM, thus passing to the corresponding state. This use case aims at exploiting the network with the actual physical conditions, that is, with reduced/actual network margins. If the monitored BER with PM-8QAM is above  $1.9 \times 10^{-2}$ , a more robust format (PM-QPSK) can be exploited (physical layer degradation use case). Once we identified these thresholds with the process outlined above, we created and installed the related FSM in the transponder.

Fig. 9 shows the content of the NETCONF <edit-conf> message sent to the transponder agent at RX to install the FSM and, thus, to instruct the transponder about the actions to perform in case of physical layer changes. The content of the message is based on the YANG model proposed in [13] and reflects the FSM of Fig. 1. One outgoing transition is present at each state: e.g., if the state is PM-8QAM (i.e., the state with “id” equal to 2) and the monitored BER  $> 1.9 \times 10^{-2}$ , a transition to the state of PM-QPSK is triggered implying

```

<finite-state-machine xmlns="http://sssup.it/fsm">
  <current-state>2</current-state>
</finite-state-machine>]]>

```

Fig. 10. Synchronization message sent by RX to TX.

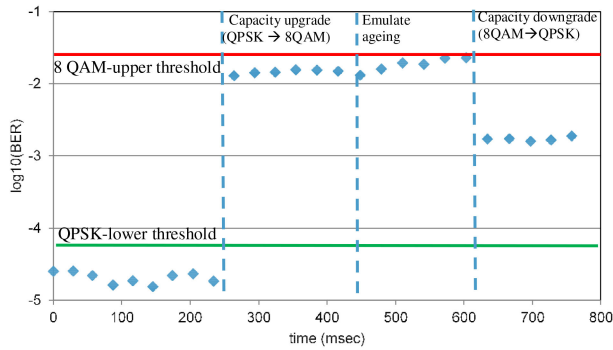


Fig. 11. Evolution of the BER during the experiment of modulation format adaptation.

$\langle \text{bit-rate} \rangle = 100$  (Gb/s) and  $\langle \text{next-state} \rangle = 1$  (which represents PM-QPSK). The threshold on the BER is expressed by the attribute  $\langle \text{threshold-param} \rangle$ , while the attribute  $\langle \text{check-operator} \rangle = \text{GT}$  (which means “greater than”) represents the check “ $\text{BER} > \text{threshold}?$ ” and  $\langle \text{check-operator} \rangle = \text{LT}$  (lower than) represents “ $\text{BER} \leq \text{threshold}?$ ”.

A connection at 100 Gb/s is initially established considering high margins (an overestimation of physical impairments), thus PM-QPSK is adopted. The monitor at the coherent receiver reveals the  $\text{BER} < 5.8 \times 10^{-5}$ , then, the transponder RX changes its state to PM-8QAM and 150 Gb/s, correcting thus the initially considered margins and being more efficient. Coordination between RX and TX has to be done to adopt the same transmission parameters, in this case the same modulation format. Thus, as assessed in Sec. II, the message shown in Fig. 10 is sent along a supervisory channel between TX and RX. This message has the format of an  $\langle \text{edit-config} \rangle$  message, which reconfigures the state of the FSM at TX, as described by Fig. 1. In particular, the state 2 corresponds to PM-8QAM.

Then, we introduced physical layer degradation with the VOA. In this case,  $\text{BER} > 1.9 \times 10^{-2}$  was measured, thus the transponder reconfigures to PM-QPSK and 100 Gb/s to maintain the service in the presence of physical layer degradations.

Fig. 11 shows the BER evolution and the successful automatic-self reconfiguration of the transponder: a low BER is first experienced; thus, the modulation format is reconfigured to PM-8QAM. Since the PM-8QAM is more spectral efficient than PM-QPSK and sensible to physical layer degradations, as expected, we observe a higher BER at this stage but within the range of acceptability. We then increase the attenuation and introduce the soft failure. As expected, the BER increases and at some point it exceeds the threshold. Then the modulation format is automatically reconfigured to PM-QPSK.

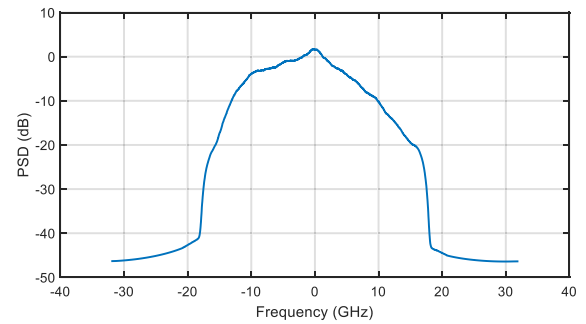


Fig. 12. Power spectral density before central frequency optimization.

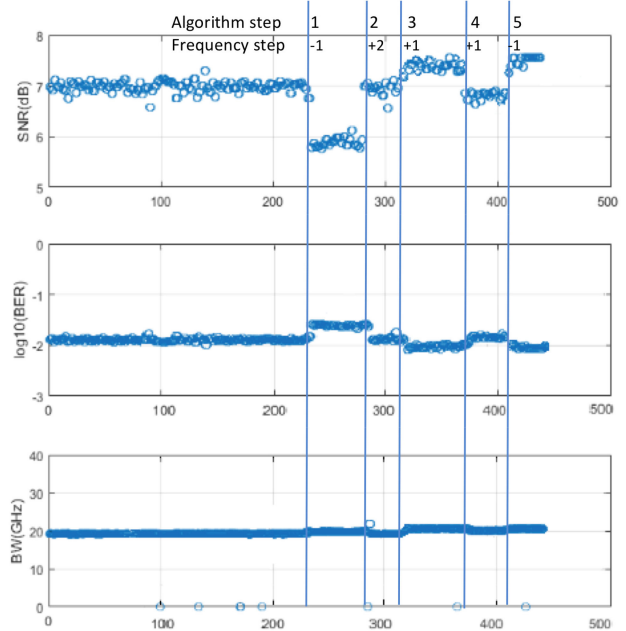


Fig. 13. Monitored SNR,  $\log(\text{BER})$ , and signal bandwidth during the optimization procedure.

## B. Optimization of the Central Frequency

In this subsection, the optimization of the central frequency is demonstrated for a lightpath with initial central frequency of 193.6 THz. To introduce distortions, the central frequency of the tunable filter before the VOA was misaligned by +2 GHz, emulating the misalignment of the TX/RX and the path filter cascade. Fig. 12 shows the power spectral density (PSD) before central frequency optimization. A distortion in the right edge of the signal is observable. Then, the following steps were performed:

- Step 0 (initial stage): 193.6 THz
- Step 1: 193.599 THz
- Step 2: 193.601 THz
- Step 3: 193.602 THz
- Step 4: 193.603 THz
- Step 5: 193.602 THz

Fig. 13 shows the monitored parameters (SNR, BER, and signal bandwidth) as a function of time. As discussed, we followed a trial-and-error process that included several steps to optimize/align the TX/RX frequency. Initially, we search around the starting frequency (by  $\pm 1$  GHz) to decide on the correct direction to move. Then we choose the direction (+) given the better performance of +1GHz than -1GHz (e.g., lower BER and higher SNR). Then at each state we monitor and obtain the average and standard deviation and when we have enough accuracy we compare with previous states in order to decide on the next move. Until 193.602 THz, performance improves. With 193.603 THz (step 4), the central frequency is shifted too much and performance is degraded (higher BER and lower SNR). Thus, we make a step back and finalize at the central frequency of 193.602 THz. In total our alignment process improved the SNR by 0.5 dB. It is also worth taking into account that a 2GHz of TX/RX and filters misalignment is considered as a reference for the ageing of the filters and lasers.

## V. CONCLUSION

We presented a field trial demonstration of a network based on finite-state-machine (FSM) control paradigm. We considered two use cases: i) pre-programmed transponder modulation format reconfiguration to enable self-adaption according to physical layer conditions, and ii) TX/RX central frequency optimization to mitigate filtering effects. The field trial demonstrated a network offering self-adaptation and automation, high flexibility, efficiency, and reliability.

Such approach on FSM can impact other operating procedures such as restoration, protection, telemetry, performance monitoring, and others that can be the subject of future works.

## REFERENCES

- [1] Y. Pointurier, "Design of low-margin optical networks," *IEEE/OSA J. Opt. Commun. Netw.*, vol. 9, no. 1, pp. A9–A17, Jan. 2017.
- [2] P. Soumplis, K. Christodouloupoulos, M. Quagliotti, A. Pagano, and E. Varvarigos, "Network planning with actual margins," *J. Lightw. Technol.*, vol. 35, no. 23, pp. 5105–5120, Dec. 2017.
- [3] M. S. Zefreh and S. Asselin, "Capacity enhancement in optical networks using margin extraction," in *Proc. Opt. Fiber Commun. Expo.*, 2018, pp. 1–3.
- [4] J. Slovak *et al.*, "Aware optical networks: Leaving the lab," *IEEE/OSA J. Opt. Commun. Netw.*, vol. 11, no. 2, pp. A134–A143, Feb. 2019.
- [5] K. Christodouloupoulos *et al.*, "Observe-decide-act: Experimental demonstration of a self-healing network," in *Proc. Opt. Fiber Commun. Conf. Expo.*, 2018, pp. 1–3.
- [6] A. P. Vela *et al.*, "BER degradation detection and failure identification in elastic optical networks," *J. Lightw. Technol.*, vol. 35, no. 21, pp. 4595–4604, Nov. 2017.
- [7] R. Martínez *et al.*, "Integrated OAM and transport SDN architecture for automatic and dynamic restoration of signal-degraded connections within flexi-grid optical networks," in *Proc. 20th Int. Conf. Transp. Opt. Netw.*, Bucharest, Romania, 2018, pp. 1–4.
- [8] A. Sadasivarao *et al.*, "High performance streaming telemetry in optical transport networks," in *Proc. Opt. Fiber Commun. Conf. Expo.*, San Diego, CA, USA, 2018, pp. 1–3.
- [9] L. Gifre, J. Izquierdo-Zaragoza, B. Shariati, and L. Velasco, "Experimental demonstration of active and passive optical networks telemetry," in *Proc. Opt. Fiber Commun. Conf. Expo.*, San Diego, CA, USA, 2018, pp. 1–3.
- [10] M. Tornatore, M. Birk, A. P. Tao Lau, Q. Zhang, and D. Zibar, "Introduction to the JOCN special issue on machine learning and data analytics for optical communications and networking," *IEEE/OSA J. Opt. Commun. Netw.*, vol. 10, no. 10, pp. ML1–ML2, Oct. 2018.
- [11] M. Filer, M. Cantono, A. Ferrari, G. Grammel, G. Galimberti, and V. Curri, "Multi-vendor experimental validation of an open source QoT estimator for optical networks," *J. Lightw. Technol.*, vol. 36, no. 15, pp. 3073–3082, Aug. 2018.
- [12] N. Sambo, F. Cugini, A. Sgambelluri, and P. Castoldi, "Monitoring plane architecture and OAM handler," *J. Lightw. Technol.*, vol. 34, no. 8, pp. 1939–1945, Apr. 2016.
- [13] M. Dallaglio, N. Sambo, F. Cugini, and P. Castoldi, "YANG models for vendor-neutral optical networks, reconfigurable through state machine," *IEEE Commun. Mag.*, vol. 55, no. 8, pp. 170–178, Aug. 2017.
- [14] L. Liu, T. Tsuritani, and I. Morita, "From GMPLS to PCE/GMPLS to OpenFlow: How much benefit can we get from the technical evolution of control plane in optical networks?," in *Proc. 14th Int. Conf. Transp. Opt. Netw.*, Coventry, U.K., 2012, pp. 1–4.
- [15] A. Giorgetti, S. Fazel, F. Paolucci, F. Cugini, and P. Castoldi, "Path protection with hierarchical PCE in GMPLS-based multi-domain WSONs," *IEEE Commun. Lett.*, vol. 17, no. 6, pp. 1268–1271, Jun. 2013.
- [16] R. Muñoz, R. Casellas, R. Vilalta, and R. Martínez, "Dynamic and adaptive control plane solutions for flexi-grid optical networks based on stateful PCE," *J. Lightw. Technol.*, vol. 32, no. 16, pp. 2703–2715, Aug. 2014.
- [17] R. Martínez, R. Casellas, R. Vilalta, and R. Muñoz, "GMPLS/PCE-controlled multi-flow optical transponders in elastic optical networks [Invited]," *IEEE/OSA J. Opt. Commun. Netw.*, vol. 7, no. 11, pp. B71–B80, Nov. 2015.
- [18] N. Sambo *et al.*, "YANG model for finite state machine," IETF Draft, 2019.
- [19] [Online]. Available: <http://openroadm.org/home.html>
- [20] [Online]. Available: <http://www.openconfig.net/>
- [21] N. Sambo, A. Giorgetti, F. Cugini, and P. Castoldi, "Sliceable transponders: Pre-programmed OAM, control, and management," *J. Lightw. Technol.*, vol. 36, no. 7, pp. 1403–1410, Apr. 2018.
- [22] N. Sambo *et al.*, "Dynamic (re)configuration of optical networks based on monitoring information: Field trial," in *Proc. OSA Photon. Netw. Devices Conf.*, Zurich, Switzerland, Jul. 2018.
- [23] F. Buchali, F. Steiner, G. Böcherer, L. Schmalen, P. Schulte, and W. Idler, "Rate adaptation and reach increase by probabilistically shaped 64-QAM: An experimental demonstration," *J. Lightw. Technol.*, vol. 34, no. 7, pp. 1599–1609, Apr. 2016.
- [24] G. Colavolpe and T. Foggi, "High spectral efficiency for long-haul optical links: Time-frequency packing vs high-order constellations," in *Proc. 39th Eur. Conf. Exhib. Opt. Commun.*, Sep. 2013, pp. 1–3.
- [25] M. Dallaglio, N. Sambo, F. Cugini, and P. Castoldi, "Control and management of transponders with NETCONF and YANG," *IEEE/OSA J. Opt. Commun. Netw.*, vol. 9, no. 3, pp. B43–B52, Mar. 2017.
- [26] F. Cugini *et al.*, "Push-pull defragmentation without traffic disruption in flexible grid optical networks," *J. Lightw. Technol.*, vol. 31, no. 1, pp. 125–133, Jan. 2013.
- [27] C. Delezoide, P. Layec, and S. Bigo, "Automated alignment between channel and filter cascade," in *Proc. Opt. Fiber Commun. Conf. Exhib.*, 2019, pp. 1–3.
- [28] A. Napoli *et al.*, "Next generation elastic optical networks: The vision of the European research project IDEALIST," *IEEE Commun. Mag.*, vol. 53, no. 2, pp. 152–162, Feb. 2015.
- [29] D. King and A. Farrel, "A PCE-based architecture for application-based network operations," IETF RFC 7491, 2015.
- [30] A. Kretsis, K. Christodouloupoulos, P. Kokkinos, and E. Varvarigos, "Planning and operating flexible optical networks: Algorithmic issues and tools," *IEEE Commun. Mag.*, vol. 52, no. 1, pp. 61–69, Jan. 2014.
- [31] R. Enns *et al.*, "Network configuration protocol (NETCONF)," IETF RFC 6241, Jun. 2011.
- [32] "Draft revised G.694.1 version 1.3," Unpublished ITU-T Study Group 15, Question 6, 2011.
- [33] [Online]. Available: <https://www.opennetworking.org/sdn-definition/>
- [34] ONF TS022, "Optical transport protocol extensions," version 1.0, Mar. 2015.
- [35] 2019. [Online]. Available: <https://wiki.onosproject.org/display/ONOS/Flow+Rules>.
- [36] R. Fielding, "Architectural styles and the design of network-based software architectures," Ph.D. dissertation, Univ. California Irvine, Irvine, CA, USA, 2000.
- [37] [Online]. Available: <https://onosproject.org/>